Global Stiffness Structural Optimization for 3D Printing Under Unknown Loads

Tuanfeng Y. Wang[1,2] Yuan Liu[1] Xuefeng Liu[3]
Zhouwang Yang[1] Dongming Yan[4] Ligang Liu[1]

[1]University of Science and Technology of China
[2]University College London
[3]Niigata University
[4]National Laboratory of Pattern Recognition, Institute of Automation, Chinese Academy of Sciences

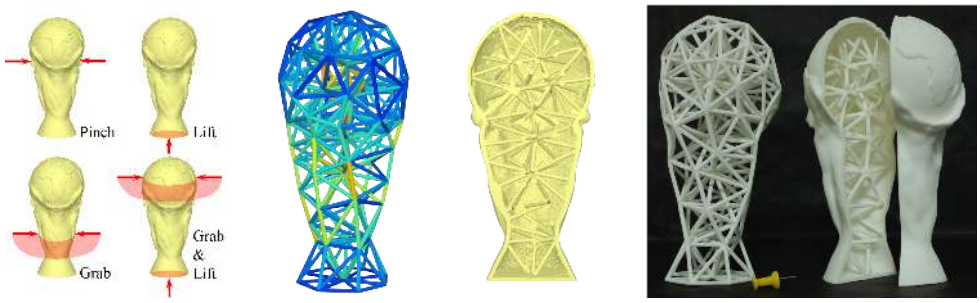

(a) (b) (c) (d)

Figure 1. A user could hold the Trophy model many possible ways (a). To be cost effective, what grips may be used should be known during the interior design, but is not. With a given amount of material, our algorithm first produces a global stiffness frame structure (b) under unknown loads, by minimizing the maximal deformation (colored according to beam radii). (c) is the sectional view of the object generated from the optimized frame structure, and (d) is the photo of the printed frame and the object generated by our method. A yellow standard pin is placed next to the object as a size reference.

Abstract

The importance of the stiffness of a 3D printed object has only been realized gradually over the years. 3D printed objects are always hollow with interior structure to make the fabrication process cost-effective while maintaining stiffness. State-of-the-art techniques are either *redundant* (using much more material than necessary to ensure the stiffness in any case) or

 ISSN 2331-7418

optimize the structure under one of the most-probable load distributions, which may fall short in other distribution cases. Furthermore, unlike industrial products using *brittle* materials such as metal, cement, etc., where stress plays a very important role in structural analysis, materials used in 3D printing such as ABS, Nylon, resin, etc. are rather elastic (*flexible*). When considering structural problems of 3D printed objects, large-scale deformation always comes before reaching stress limits when loads are applied. We propose a novel approach for designing the interior of an object by optimizing the global stiffness — minimizing the maximum deformation under any possible load distribution. The basic idea is to maximize the smallest eigenvalue of the stiffness matrix. More specifically, we first simulate the object as a lightweight frame structure, and optimize both the size and the geometry using an eigen-mode-like formulation, interleaved with a topology clean. A postprocess is applied to generate the final object based on the optimized frame structure. The proposed method does not require specific load cases and material strengths as inputs, which the existing methods require. The results obtained from our experiments show that optimizing the interior structure under unknown loads automatically keeps strength where the structure is the weakest and is proven to be a powerful and reasonable design framework.

1. Introduction

3D printing techniques provide a powerful solution for prototyping custom objects with fine surface details and complex interior structures. However, the spread and development of this technique is hindered by the high cost of material and low speed of fabrication. Research efforts have been devoted to ways to reduce the material used, i.e., the volume/weight of object. The key challenge here is to keep the stiffness while using less material. Given a load distribution, it is natural to hollow the object to be more cost-effective, and add interior structure to optimize the structural stiffness-to-weight ratio [Stava et al. 2012; Wang et al. 2013; Lu et al. 2014; Zhang et al. 2015]. Such load-distribution-based techniques have been highly successful in ideal cases, perfectly minimizing the structural deformation/stress under corresponding preset loads with much less material. However, they are not suitable for many real world applications because the loads on a fabricated object may appear in other distributions, which are different from the preset one. As shown in Figure 1(a), the Trophy model could be held in many different ways, which leads to very different load distribution cases.

Instead of taking one (or several) load distribution case(s) into consideration, we optimize the global stiffness-to-weight ratio by minimizing the maximum deformation under any load distribution. This is known as *unknown load* due to having no load distribution case given. We use the criterion *deformation* rather than *stress*, as the former is more suitable when using elastic materials like those used in 3D printing. The elastic property prevents the fabricated object from breaking under large stress,

but is much easier to deform when load is applied. The rationale of the deformation based formulation is also supported by previous research (see Sec. 3.3). When the amount of material is given, our unknown-load-based optimization framework aims to make the object perform the best (stiffest) among possible interior designs, when the corresponding worst (leading to the largest deformation) load distribution case is applied.

Our work is inspired by the research of Chen [2007] and Wang et al. [2013]. These studies show that an entire object can be simulated by a frame structure consisting of a set of beams and a set of nodes connected by these beams. A frame structure captures most of the structural features of the object and has a rather small set of parameters which can be analyzed and computed with high efficiency. Furthermore, frame structures are more flexible in design than simple hollowing while being much easier to clean inner unused material (in SLS, SLA, etc.) than cell structures. The last step of our framework restores the optimized frame structure back into the object, ready to be fabricated while preserving the global stiffness property.

Prior to global stiffness optimization, we first perform a *Constrained Centroidal Voronoi Tessellation* (CCVT) on the input object, and obtain an isotropic initial frame by taking the edges of each tetrahedron as a beam of the initial frame. The global stiffness problem is then formulated as a saddle point problem, minimizing the maximum norm of the deformation under any normalized load. Optimization on nodes positions, beam radii and nodes topology connections are applied to the frame structure using a saddle point algorithm. After the optimization algorithm is terminated, we adopt a postprocess step to generate the object with original object surface and lightweight interior based on the optimized frame structure. Note that this is not simply placing a skin over the frame structure as done by Wang et al. [2013]. As the skin can not be analyzed efficiently, our postprocess is rather like an adaptive hollowing while adding interior supportive structure. Finally, we use the *Finite Element Method* (FEM) to analyze and verify the rationality of our results.

2. Related Work

In recent years, significant efforts have been made on fabrication-aware 3D shape design, for physically-fabricated prototypes and manufactured objects using 3D printing. Previous work focused on the desire for certain physical properties, such as deformation behaviour [Bickel et al. 2010], ability to be fabricated via commercial 3D printer's limited working volume [Luo et al. 2012], physical realization [Stava et al. 2012], or stability over gravity in certain orientations [Prévost et al. 2013; Bächer et al. 2014]. These studies fully developed the benefit of 3D printing over traditional CNC fabrication techniques, because both fine surface details and complex interior structure can be fabricated.

Over the recent years it has been more and more recognized that 3D printing techniques, including FDM/SLS/SLA, etc., are hindered due to high material cost and a rather low fabrication speed. The core problem is to reduce the designed volume of the object. Inspired by lightweight structure observed from nature, Wang et al. [2013] and Lu et al [2014] adopted lightweight structures to fill the object rather than a solid interior. These studies optimize the stiffness and strength-to-weight ratio under a given external force while the original object surface is preserved. However, the results of these load-based methods fall short in real world cases, as load distributions applied by a user is always different from the ideal preset case. With a novel formulation, our proposed unknown-load-based method perfectly solves this problem by optimizing and generating a global stiffness design with a uniform framework. Without a given load distribution, Umetani and Schmidt [2013] present a structural analysis technique that slices the object into cross-sections and computes stress based on bending momentum equilibrium. For a similar purpose, a finite element based structural analysis method is presented by Zhou et al. [2013]. Based on experimental observation, this work uses an Eigenmode formulation to detect the weakest area of an object. In our paper, this observation is proved mathematically from our global stiffness formulation. In the computational structure area, structural analyses and optimization under unknown load distribution have been discussed during the past few years [Cherkaev and Cherkaev 2004; Cherkaev and Cherkaeva 1999; Takezawa et al. 2011]. These studies, although sharing the same target, test different kinds of object functions without a proof of rationality. These studies also limited the problem to a 2D domain, and focus on only geometry rather than taking all the variables (size, geometry, topology) into consideration, which is far from a complete solution of the cost-effective fabrication challenge.

In order to reduce the volume of the object, a lightweight structure is adapted for supportive interior. The design and optimization of lightweight structures have been extensively explored in tissue engineering and computer-aided design. Smith et al. [2002] focus on optimizing the design of truss structures where beams connected by pin joints are rotation-free making it difficult to preserve the geometric shape of the object. Using lightweight structures for improving the strength and the stiffness of objects has also been studied in the field of rapid manufacturing [Wang et al. 2005], where particle swarm optimization and generic algorithms have been used to search for design solutions. Detailed reviews on various aspects of structural optimization can be found in Bendsoe and Sigmund [2003]. Due to the differences in the types of objectives and constraints, these approaches are not suitable for our purpose in 3D printing.

We use the frame structure in the lightweight design because it is fabrication friendly. Each beam in the frame structure is considered as a basic element, which is different from classical structural topology optimization methods. Structural topology

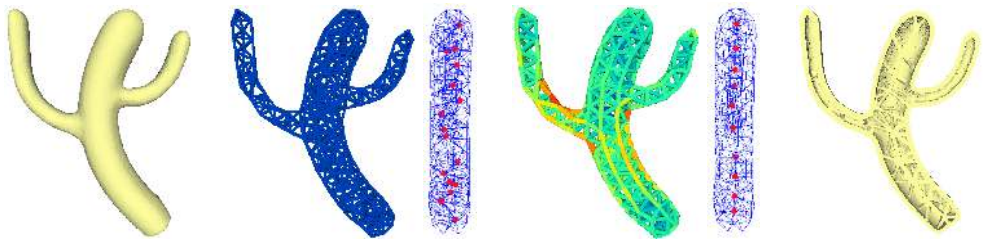

(a) (b) (c) (d)

Figure 2. Pipeline of our approach. Given an input model (a), an initial frame structure (b) is generated. Our method runs a saddle point algorithm to obtain an optimized frame structure (c) which provides minimal deformation under unknown load distribution. (c) is colored to visualize the radii and a side view of the frame structure is presented to show the node position and topology connections before and after optimization. Then a post-processing step is applied to generate a solid structure (d) for 3D printing. The front part of (d) is removed in order to show the internal structure.

optimization is employed mainly to specify the optimum number and location of holes in the configuration of the designed structure. Different classes of approaches have been studied in past such as evolutionary structural optimization [Xie and Steven 1997; Huang and Xie 2010]. Element-based methods for structural topology optimization decompose the volume of the input object into finite-element-like tetrahedrons, or a grid-like structure for analysis. The *Optimality Criteria* (OC) [Rozvany 1989] methods have proven to be among the most effective element-based methods for solving topology optimization problems. A recent review of this area is offered by Rovanzy [2009]. It is easy to extend our framework into element-based computation, however, due to the linear elastic property of the frame structure, taking a single beam as the basic element is much more efficient.

3. Problem and formulation

Problem. The input to our framework is the surface mesh, S. Our goal is to generate an entity global stiffness object model, H, consisting of an adaptive hollowed shell and a supportive interior structure, while utilizing no more than a given amount of material. The generated object shares the same surface with as S, but has much less weight than S since it has a lightweight supportive structure rather than being solid filled.

Remarks The following two problems are usually considered in structural optimization: Stiffness-to-Weight and Weight-to-Stiffness. The Stiffness-to-Weight problem is to design a structure with the maximum stiffness using a specific amount of given material; and the Weight-to-Stiffness problem is to design a structure with the least

amount of material, but satisfied the given stiffness expectation. These two problems are dual and can be converted to each other by a simple binary search process. Without loss of generality, here we focus on the former one that takes the amount of material use as the constraint. We also consider the load only from external forces, as the internal forces such as gravity remain very small compared with external forces.

3.1. Frame structure

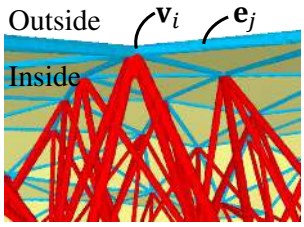

A frame structure, $\mathcal{T}$, consists of a set of frame nodes, $V = \{\mathbf{v}_i, i = 1, 2, \cdots, m\}$, which are sampled on S (marked in yellow) and in the volume enclosed by S, as well as a set of frame beams, $E = \{\mathbf{e}_j, j = 1, 2, \cdots, n\}$, which are the edges connecting the nodes, as shown in the figure to the right. Each node, $\mathbf{v}_i$, represents a geometric position and each beam, $\mathbf{e}_j$, is a cylindrical shape with radius r_j and length l_j. Here $\mathcal{T}$ can be seen as a graph of V and E with the geometry defining node positions, the beam radii, and the topology defining the connectivity between nodes. For convenience, we also denote $V_S = \{\mathbf{v}_i \mid \mathbf{v}_i \in S\}$, $V_I = V \setminus V_S$, $E_S = \{\mathbf{e}_j \mid \mathbf{e}_j \in S\}$ (marked in cyan), and $E_I = E \setminus E_S$ (marked in red).

By taking adequate density of surface points, the appearance of frame $\mathcal{T}$ is expected to approximate S within a certain geometric error [Yan et al. 2009]. After the frame is optimized, surface edges of frame (E_S) indicate the adaptive thickness (doubled radius) of the surface shell around the position of the edges. Interior edges of the frame (E_I) are taken as cylinder-like supportive beams. Then the frame $\mathcal{T}$ can be considered as a reasonable approximation of the final entity object $\mathcal{H}$.

The approach presented in this paper uses node positions and beam radii as design variables in the global stiffness structural optimization. This is different from element-based methods for structural topology optimization [Rozvany 2009], where problems are expressed by tetrahedron-element-wise step functions. As an effective discrete representation, the frame structure is fabrication-friendly and has simple mechanical properties which will be described in Section 3.2.

3.2. Stiffness matrix

The mechanics of frame structure has been studied based on beam theory [Hughes 1987; Gibson and Ashby 1999; Chandrupatla et al. 1991], where frame beams are assumed to behave like simple beams under linear deformation caused by nodes' displacement or rotation. In our method, we make the following assumptions in calculating the equilibrium state of the structure.

a) The beams are only connected to each other at nodes.

b) The beams are connected rigidly to have tensile, torsion, transverse shear force.

c) Each node has three displacement degrees of freedom and three rotation degrees of freedom.

Linear relationship between deformation and force For a given frame structure, including both the surface and interior beams, the relationship between deformation —the displacement and rotation of each node, and the force (including torque) should satisfy the following discretized equilibrium equation.

$$K(V, \mathbf{r})D = F, \tag{1}$$

where $V = (\mathbf{v}_1, \cdots, \mathbf{v}_m)$ also denotes the geometric positions of the nodes. $K(V, \mathbf{r})$ is the stiffness matrix, which depends on node positions V and beam radii, $\mathbf{r} = (r_1, \cdots, r_n)$. $F = (\mathbf{f}_1, \cdots, \mathbf{f}_m)^T$ is the force and torque distribution acting on each node and $D = (\mathbf{d}_1, \cdots, \mathbf{d}_m)^T$ is the displacement and the rotation of deformation caused by F. For details, please refer to Chandrupatla et al. [1991]. Note that F in Eq. (1) is the sum of external force and only acts on a set of nodes in V_S. This is for a better simulation of real world cases because external forces always act on the surface.

3.3. Eigen-Mode-like formulation

Our global stiffness target, which minimizes the maximum deformation under unknown loads can be described as an Eigen-Mode-like formulation.

Originally, for the frame structure simulated from an object, we first find an external force, F, that gives the maximal deformation. In order to avoid the scale problem, it is estimated by a deformation ratio, $(D^T D)/(F^T F)$. Then we minimize the maximal deformation ratio of the frame structure by varying the design variables, $(V_I, \mathbf{r})$.

For an object in the state of equilibrium, the following conditions for F are needed:

$$\mathbf{1} \cdot F_i = 0, \quad F_i \cdot (X_{i+1} - X_{c,i+1}) - F_{i+1} \cdot (X_i - X_{c,i}) = 0 \tag{2}$$

where $i = 1, 2, 3$; F_1, F_2, F_3 are force components of F along x, y, z axis respectively; X_1, X_2, X_3 are the lists of x-, y-, z-coordinates of the nodes X in a fame structure; $X_c = (X_{c,1}, X_{c,2}, X_{c,3})$ is the center point of the object. These two constrains indicate that both the force and the moment of the force are zero. Since stiffness matrix K is singular, for each F satisfying Eq. (2), to uniquely determine a solution $KD = F$, the translation and rotation should be ignored. Similar to Eq. (2), the total displacement and the total moment of displacement, the total rotation and the total moment of rotation are set to zero. Let the stiffness matrix under the above conditions on force and deformation be $\hat{K}$, which is now a regular matrix, then we have $D = \hat{K}^{-1}F$.

Thus, the structural optimization problem can be constructed as follows

$$\min_{(V_I,\mathbf{r})\in\Theta} \quad \max_{F \text{ satisfying } (2)} \frac{(\hat{K}^{-1}F)^T(\hat{K}^{-1}F)}{F^TF} \tag{3}$$

where Θ is the collection of all feasible V_I and $\mathbf{r}$; see detailed constrains in Sec. 3.4. This formulation is not easily solvable [Li et al. 2015], and needs to be cast into a Rayleigh-quotient optimization which will be discussed in detail later in Section 4.2.

Eigen-Mode property Here we discuss a more general situation if the external force can also act on V_I. As the stiffness matrix $\hat{K}$ is symmetric, the vector F that maximizes the value $(\hat{K}^{-1}F)^T(\hat{K}^{-1}F)/F^TF$, according to Parlett [1998], is just the eigenvector corresponding to the smallest eigenvalue of $\hat{K}$, denoted by $\lambda_{\min}(\hat{K})$ which is actually the same as the minimal positive eigenvalue of K. Finally, we have such an eigen-mode optimization problem

$$\max_{(V_I,\mathbf{r})\in\Theta} \quad \lambda^*_{\min}(K(V,\mathbf{r})) \tag{4}$$

where $\lambda^*_{\min}(K(V,\mathbf{r}))$ is the minimal positive eigenvalue of stiffness matrix $K(V,\mathbf{r})$.

In this way, our formulation mathematically proves the observation given by Zhou et al. [2013] that the eigenvector of a kinematic equation indicates a structural worst-case. Here our linear relationship between deformation and force (ignoring the first derivative of force) is a static but more realistic version of the kinematic equation. Our global stiffness optimization, therefore, can also be considered to automatically reinforce where the structure is the weakest. On the other hand, plenty of physical experiments done by Zhou et al. [2013] can also show that our deformation-based formulation is reasonable in calculating a 3D Printed object.

3.4. Constraints on structure design parameters

Radius bounds To make the frame structure printable, the radius of each beam should be no less than the minimum printable radius, $\underline{r}$. To avoid unrealistic design, an upper bound, $\overline{r}$, for the radius is imposed for each beam. Moreover, in order to retain the linear elastic property of the frame structure, the ratio between the length and the radius of a beam must satisfy the Euler buckling constraint. In brief, the buckling and the printability can be integrated as a bounded constraint for each beam radius

$$\underline{\eta}_j \leqslant r_j \leqslant \overline{r}, \quad \mathbf{e}_j \in E, \tag{5}$$

where $\underline{\eta}_j = \max(l_j/\alpha, \underline{r})$, l_j is the length of beam $\mathbf{e}_j$, and α is the slenderness ratio.

Volume The proposed problem is defined as optimizing the frame structure when a certain amount of material is given.

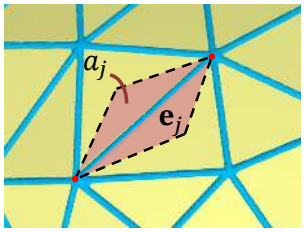

Let $\overline{\text{Vol}}$ be the amount of material available. The volume of solid material in the designed structure, $\mathcal{H}$, consists of two parts: the volume of interior beams in the frame, and the volume of an adaptive-hollowed shell, which can be approximately calculated as the sum of the product of the area covered by a surface beams and its doubled radius. Thus we have a constraint on the material volume

$$\sum_{\mathbf{e}_j \in E_I} \pi {r_j}^2 l_j + \sum_{\mathbf{e}_j \in E_S} 2 r_j a_j \leqslant \overline{\text{Vol}}, \tag{6}$$

where a_j is the area covered by beam $\mathbf{e}_j$ on the surface. In practice, a_j is roughly calculated as the shaded area shown on the right.

Shape barrier The appearance of our optimal result should be the same as the surface of the input mesh. As a result, elements in internal beams set E_I have to be kept inside of the volume enclosed by S. Many algorithms have been developed for this purpose. In our implementation, an efficient but approximate method is adopted in which several test points are sampled from each beam for a quick check whether they are inside S. A feasible solution of the optimization problem is subject to the constraint that all the test points are inside S.

Other constrains The objective function of our optimization is very flexible and can be solved efficiently. As a result, addition constrains are able to be considered in our formulation such as stability, self-supportiveness, orientation, angle of beams, etc., including printability constrains specified by certain printing techniques. In this paper, we focus on the main problem – global stiffness formulation, as these constrains have been well studied by many previous works [Wang et al. 2013].

4. Methodology

We propose a novel approach for solving Eq. (3) – finding a global stiffness structure which provides the best load-bearing performance under any possible load distribution. An overview of our algorithm is shown in Figure 2. Given a closed 3D input surface S represented by a triangular mesh, we first compute an isotropic initial frame with its beams of lower radii bound. We use the *Constrained Centroidal Voronoi Tessellation* (CCVT) [Yan et al. 2010] for this step (see Figure 2(b) for an example). Starting from this initial frame, we then iteratively optimize the beam radii and node position by solving a saddle point problem (see Figure 2(c)), to achieve a frame with maximum global stiffness under the volume constraint. Finally, we apply a post-processing step to the optimized frame structure to generate an entity object that inherits the global stiffness property as the final result (see Figure 2(d)).

4.1. Frame initialization

For our purpose, we chose an isotropic tetrahedralization approach [Yan et al. 2010] to guide the frame initialization, with a uniform density function. We first randomly generate a set of sites in the interior domain of surface S. The number of sites is specified by the user, it is related to the complexity of frame structure. Then, we minimize the CCVT energy function by iteratively optimizing the positions of the sites. Once the optimization is terminated, the dual triangulation is extracted as the initial frame. This initial frame will be determined by having each tetrahedral edge as a frame beam with the radius $\underline{\eta}$ (defined in Eq. (5)). Although an adaptive initialization of the starting point can often benefit optimization, it is actually ill-posed as our target is to strengthen the weakest parts of the structure. The weakest situation changes during optimization (see Figure 4), so adaptive initialization for the *initial* weakest situation will not benefit the final result. On the other hand, an isotropic initialization is good enough as our geometry optimization is shown to contribute a lot to the final result (see Figure 2(d)). It also worth mentioning that final result is not sensitive to the number and location of initial sites because our optimization will both move sites and remove redundant ones.

Remarks For thin details on the surface, damage can easily happen even without any hollowing. So as a part of the initialization, we first simplify all the thin parts, and then add these geometric details back only after the solid object is finally generated. This is automatically realized thanks to the natural limitation of CCVT, which eliminates thin parts by optimizing the energy function with a uniform density function. To add geometry detail back, we can simply use the original mesh as outer surface instead of the outer surface formed by CCVT mesh. Therefore, the final result should have the exact same appearance with the input surface mesh S.

4.2. Saddle point algorithm

In the global stiffness structural optimization, Eq. (3), derivatives of the objective function, e.g., gradients with respect to V_I and $\mathbf{r}$, cannot be explicitly expressed and efficiently calculated. It would be extremely unfavorable to employ most iterative strategies that make use of the first and probably second derivatives of the objective function. However, without using gradient information, the computational cost of using direct search methods would be too expensive and time-consuming. Through rigorous mathematical derivation, we will present an algorithm based on the Rayleigh quotient to greatly accelerate the solving of the problem.

We first define the Rayleigh quotient [Parlett 1998] of the stiffness matrix $K(V, \mathbf{r})$ as

$$Q(V, \mathbf{r}, \mathbf{u}) = \frac{< K(V, \mathbf{r})\mathbf{u}, \mathbf{u} >}{< \mathbf{u}, \mathbf{u} >}. \tag{7}$$

According to the properties of Rayleigh quotient, the global stiffness structural opti-

mization Eq. (3) is equivalent to the following saddle point problem

$$\max_{(V_I,\mathbf{r})\in\Theta} \quad \min_{\mathbf{u}\in N(K)^{\perp}} \quad Q(V,\mathbf{r},\mathbf{u}) \tag{8}$$

where $N(K)^{\perp} = \{\mathbf{u} \mid \mathbf{z}_i^T\mathbf{u} = 0, i = 1,\cdots,6\}$ is the orthogonal complement of $Null(K) = \text{span}\{\mathbf{z}_1,\cdots,\mathbf{z}_6\}$. Note that it is not necessary to compute $\mathbf{z}_i$ or $N(K)^{\perp}$ explicitly as we always take $\mathbf{u}$ as the minimal positive eigenvalue. In the saddle point problem in Eq. (8), the gradients $\{\nabla_V Q, \nabla_{\mathbf{r}} Q, \nabla_{\mathbf{u}} Q\}$ have explicit expressions and can be computed efficiently. Thus, we can design a Rayleigh-quotient based algorithm for optimizing the frame structure as follows.

Algorithm 1 Rayleigh-quotient based algorithm

Input: an initial frame $\mathcal{T}^{(0)}$ obtained in Section 4.1

Output: an optimized frame $\mathcal{T}$ with its design variables $(V_I, \mathbf{r})$

Step 1: Get $(V^{(0)}, \mathbf{r}^{(0)})$ from the initial frame, obtain the eigenvector $\tilde{\mathbf{u}}^{(0)}$ corresponding to the minimal positive eigenvalue of $K(V^{(0)}, \mathbf{r}^{(0)})$, specify a threshold ϵ, and let $k := 1$.

Step 2: Update $(V_I^{(k)}, \mathbf{r}^{(k)}) = \arg\max_{(V_I,\mathbf{r})\in\Theta} Q(V, \mathbf{r}, \tilde{\mathbf{u}}^{(k-1)})$ by the interior-point algorithm [Nocedal and Wright 2006, Chapter 19].

Step 3: Compute the minimal positive eigenvalue of $K(V^{(k)}, \mathbf{r}^{(k)})$ and its corresponding eigenvector $\tilde{\mathbf{u}}^{(k)}$.

Step 4: If $Q(V^{(k)}, \mathbf{r}^{(k)}, \tilde{\mathbf{u}}^{(k)}) - Q(V^{(k-1)}, \mathbf{r}^{(k-1)}, \tilde{\mathbf{u}}^{(k-1)}) \leq \epsilon$, then output $(V^{(k)}, \mathbf{r}^{(k)})$ as optimized design variables for the final frame; Otherwise, go back to **Step 2**.

When the optimized frame is generated from our Rayleigh-quotient based algorithm, we will then merge any pairs of nodes that are connected by a strut that is at the minimum allowable length. The struts with small radii can also be eliminated to simplify the structure by applying a sparse optimization described in Wang et al. [2013]. After this topology-cleaning step, we will use the optimized frame to generate a solid structure $\mathcal{H}$ for 3D printing.

4.3. Postprocess

The ultimate goal of our approach is to generate an entity object H inside the surface boundary S. For this purpose, we separate the optimized frame $\mathcal{T}$ into the boundary beam set E_S and the interior beam set E_I, as discussed in Section 3.1. The beam sets E_S and E_I will guide the adaptive hollowing and interior structure generation, respectively.

First, the radii of the surface beams are used to determine a thickness function as

$$\zeta(\mathbf{p}) = 2(w_1 \cdot r_{j_1} + w_2 \cdot r_{j_2} + w_3 \cdot r_{j_3}),\ \forall \mathbf{p} \in S,$$

where $\{r_{j_1}, r_{j_2}, r_{j_3}\}$ are the radii of three surface beams from triangle $\triangle \mathbf{e}_{j_1}\mathbf{e}_{j_2}\mathbf{e}_{j_3} \subset E_S$ where the point $\mathbf{p}$ lies, and $\{w_1, w_2, w_3\}$ are its barycentric coordinates. Let $\Omega \subset \mathbb{R}^3$ be the region bounded by the input surface mesh S. Then the adaptive hollowed surface shell is defined as

$$H_S = \{\mathbf{q} \in \Omega \mid \|\mathbf{q} - \mathbf{p}\| \leqslant \zeta(\mathbf{p}),\ \forall \mathbf{p} \in S\}, \tag{9}$$

which can be considered as a piecewise linear interpolation of the surface beams E_S. Similarly, the beams in E_I are used to define the interior supportive structure as

$$H_I = \{\mathbf{q} \in \Omega \mid \mathrm{dist}(\mathbf{q}, \mathbf{e}_j) \leqslant r_j,\ \forall \mathbf{e}_j \in E_I\}, \tag{10}$$

where $\mathrm{dist}(\mathbf{q}, \mathbf{e}_j)$ is the geometric distance of point $\mathbf{q}$ to the line segment $\mathbf{e}_j$. The whole solid structure H can then be given as

$$H = H_S \bigcup H_I.$$

Finally, we apply the *Extended Dual Contouring* (EDC) algorithm [Wang and Chen 2013] to extract the 2-manifold surface boundary of solid H. As shown in Figure 2(d), the generated solid structure with its boundary mesh is now ready for 3D printing.

5. Results and discussion

Our approach offers a global stiffness design of interior structure given the input surface mesh and the amount of material allowed. Our algorithm is applied to a variety of objects with different load distributions in regular use including an American football, toys and models. We first verify the optimization results of our formulation with the analysis framework in Sec. 3.2, and then verify the final results of the whole framework, which are generated based on the optimized frame structures. This is different from verifying the result of optimization under given load. Our global stiffness optimization result is difficult to test in real physical experiments but thanks to the advance of FEM techniques, we examed our results based on a FEM-based computational framework that is considered as a good simulation of physical experiment.

Criteria With a $10N$ load is applied, two criteria are discussed here: *Average* deformation and *Maximum* deformation. 4000 random load distribution cases are applied. The *Average* is the mean value of the norm of the 4000 deformations produced by corresponding load distributions. The *Maximum* deformation is obtained by applying the load that leads to the maximum norm of deformation on the frame structure to

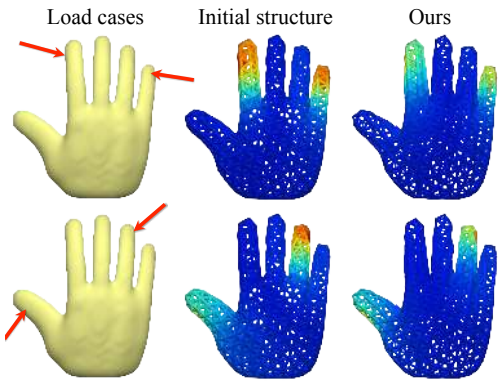

Figure 3. Deformation distribution of two load distribution cases (top and bottom row) on the initial structure (center) and our optimized structure of hand model (right). The red arrows shown on the left model indicate pair of forces used to simulate the deformation. The initial structure we tested has the same volume with our result. Warmer color refers to a larger deformations and cooler color refers to a smaller deformations. It is obvious that our result performed better in these two selected cases.

the final object. This is the load distribution given by the inner optimization of our formulation, i.e.,

$$\max_{F \text{ satisfying } (2)} \frac{(\hat{K}^{-1}F)^T(\hat{K}^{-1}F)}{F^TF}.$$

The load distribution is given by the result of Zhou et al. [2013]. In our experiments, the amount of material use is set to 20% of the solid volume of the input object. The better global stiffness property, the less value these two criteria provide.

To verify the global stiffness property of our optimized frame structure, we compare the initial structure with uniform beam radii. The uniform radii is set to make the control structure have the same volume as our result. In Figure 3, two cases of the hand model are presented where warmer color refers to a larger value of deformation and cooler color refers to a smaller value of deformation. The map of the *Maximum* deformation for all the tested models is shown in Figure 4. With the statistic data in Table 1, our proposed formulation is shown to be able to optimize the global stiffness of a given initial frame structure.

Physical experiment simulation To examine the final object generated based on the optimized frame structure, a FEM-based computation framework is adopted. For an elastic body Ω, the stationary state of objects under forces can be described by the

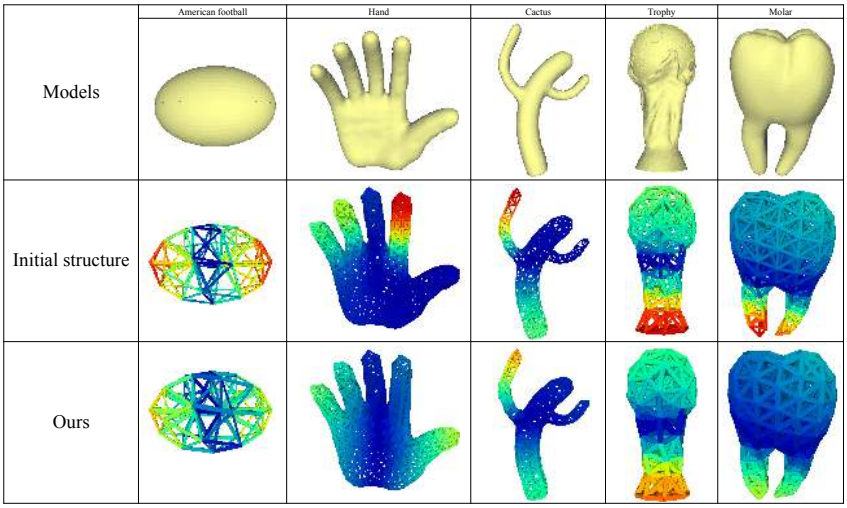

Figure 4. Maximum deformation distribution cases for each test frame structure. Top: Input model; Middle: distribution map of deformations for the initial structure; Bottom: distribution map of deformations for our optimized structure. The magnitude of maximum deformation on our resulting structure is much smaller than that on the uniform initial frame structure. Note that, for example in the hand model, the worst case changes during our optimization of the frame structures.

Table 1. Statistics of frame structure tests. Mean values of 4000 deformations (in mm) for each model are listed. The maximum deformation value for each model is also listed. First two rows are the results for a uniform frame and the last two rows are our results.

Models		American football	Hand	Cactus	Trophy	Molar
Initial structure	*Avg.*	0.198	0.677	0.781	0.110	0.141
	Max	0.273	1.083	1.264	0.269	0.233
Ours	*Avg.*	0.193	0.523	0.516	0.106	0.101
	Max	0.256	0.790	0.832	0.258	0.154

linear elasticity problem,

$$\begin{aligned} -\text{div}(\sigma(\epsilon(u))) &= f, \quad in\ \Omega \\ u &= 0, \quad on\ \Gamma_D \\ \sigma(\epsilon(u)) \cdot n &= g, \quad on\ \Gamma_N. \end{aligned} \tag{11}$$

In this problem, u is displacement, $\epsilon(u) = 1/2(\nabla u + \nabla u^T)$ is the strain, and $\sigma(\epsilon) = 2\mu\epsilon + \gamma(\text{tr}(\epsilon))I$ is the stress. The quantities γ and μ are the Young's modulus and shear modulus of the material (also known as Lame moduli). Such a problem can be solved by using FEMs. In our experiment, the FEM computation were obtained using DOLFIN [Logg et al. 2012].

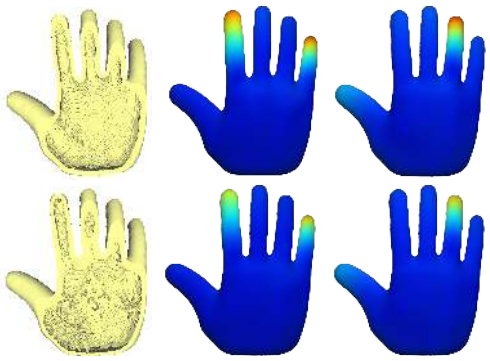

Figure 5. Deformation distribution of the same two load distribution cases shown in Figure 3 on the uniform hollowing result (top) and our optimal result (bottom) for the hand model. The first column is the sectional view. The load is acted as pinching the forefinger and the little finger for the second column and pinching the thumb and the third finger for the last column. Two objects tested have the same volume. It can be observed that the final object generated by our proposed postpocessing can successfully inherit the mechanical properties and preforms better.

Table 2. Statistics of the simulation tests for each object. Mean values of 4000 deformations (in mm) for each model are listed. The maximum deformation value for each model is also listed. First two rows are the results of the uniform hollowing solution and the last two rows are our results.

Models		American football	Hand	Cactus	Trophy	Molar
Uniform hollowing	*Avg.*	0.138	1.135	1.259	0.998	0.287
	Max	0.201	1.529	2.165	1.486	0.469
Ours	*Avg.*	0.121	0.972	1.029	0.626	0.106
	Max	0.189	1.347	1.768	1.097	0.158

We compare our results to a uniform hollowing solution. In Figure 5, we show the comparison of the same cases as shown in Figure 3 for the hand model. Explicit statistic data for all tested models is shown in Table 2. We also compare our result with Lu et al. [2014]. We generate a global stiffness molar model which has the same volume as the molar example provided by this work as shown in Figure 6. The simulated results show that ours are more suitable under unknown load cases.

Our saddle point optimization problem can be solved very efficiently. All examples appear in this paper are optimized within 20 minutes on a PC running Linux OS with a 2.8GHZ Core CPU and 8GB RAM.

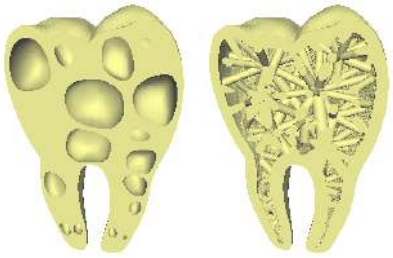

Figure 6. We compare our result with Lu et al. [2014]. The left one is provided by Lu et al. [Lu et al. 2014] and the right one is ours. Two result objects have the same volume and the (Avg., Max) deformation is (0.125,0.197) and (0.106,0.158), respectively.

Figure 7. We fabricate the final results for some models.

6. Conclusion

In this work, we proposed a novel approach for global stiffness structure optimization and present a saddle point algorithm to solve the optimization problem efficiently. When given a certain amount of material for printing an object in 3D, our approach can generate a global stiffness structure with minimum deformation under all possible force distributions. Furthermore, our approach provides a solution for formulating adaptive hollowing and interior supportive structures in a unified form, while optimizing them simultaneously. A number of experimental results have shown the validity and the rationality of our solution, and proved our proposed approach to be much more applicable than previous methods.

Limitations and future work Our research opens several future studies in the direction of structural optimization.

The optimization objective of this paper was to minimize the possible deformation of objects. However, the maximum stress distribution inside an object is of more interest in some applications, since it tells us where a crack is likely to happen. For such a need, we should introduce new objective functions. A simple idea is to consider

the following optimization problem,

$$\min_{(V,r)} \max_{f} \frac{\int_\Omega |\sigma|^2 dx}{\int_\Omega f^2 dx}$$

where σ denotes the stress of the body under a force f.

Acknowledgements

This work is supported by the National Natural Science Foundation of China (Nos: 61222206, 11371341, 11526212, 61372168, 61271431), the Fundamental Research Funds for the Central Universities (WK0010000051), and the One Hundred Talent Project of the Chinese Academy of Sciences.

References

BÄCHER, M., WHITING, E., BICKEL, B., AND SORKINE-HORNUNG, O. 2014. Spin-it: optimizing moment of inertia for spinnable objects. *ACM Transactions on Graphics (TOG) 33*, 4, 96. URL: http://dx.doi.org/10.1145/2601097.2601157. 20

BENDSOE, M. P., AND SIGMUND, O. 2003. *Topology optimization: theory, methods and applications*. Springer. 21

BICKEL, B., BÄCHER, M., OTADUY, M. A., LEE, H. R., PFISTER, H., GROSS, M., AND MATUSIK, W. 2010. Design and fabrication of materials with desired deformation behavior. *ACM Trans. Graph. 29*, 4 (July), 63:1–63:10. URL: http://doi.acm.org/10.1145/1778765.1778800, doi:10.1145/1778765.1778800. 20

CHANDRUPATLA, T. R., BELEGUNDU, A. D., RAMESH, T., AND RAY, C. 1991. *Introduction to finite elements in engineering*. Prentice-Hall Englewood Cliffs, NJ. 23, 24

CHEN, Y. 2007. 3D texture mapping for rapid manufacturing. *Computer-Aided Design and Applications 4*, 6, 761–771. URL: http://www-bcf.usc.edu/~yongchen/Research/3DTextures.pdf. 20

CHERKAEV, E., AND CHERKAEV, A. 2004. Principal compliance and robust optimal design. In *The Rational Spirit in Modern Continuum Mechanics*. Springer, 169–196. URL: http://www.math.utah.edu/~cherk/publ/uncertain.pdf. 21

CHERKAEV, A., AND CHERKAEVA, E. 1999. Stable optimal design for uncertain loading conditions. *Homogenization (V. Berdichevsky, V. Jikov and G. Papanicolaou, Eds.), World Scientific*, 193–213. URL: http://www.math.utah.edu/~cherk/publ/opt_load.ps. 21

GIBSON, L. J., AND ASHBY, M. F. 1999. *Cellular Solids: Structure and Properties*, 2nd ed. Cambridge University Press. 23

HUANG, X., AND XIE, M. 2010. *Evolutionary topology optimization of continuum structures: methods and applications*. John Wiley & Sons. 22

HUGHES, T. J. R. 1987. *The Finite Element Method: Linear Static and Dynamic Finite Element Analysis*. Prentice-Hall. 23

LI, Y., XIE, X., AND YANG, Z. 2015. Alternating direction method of multipliers for solving dictionary learning models. *Communications in Mathematics and Statistics 3*, 1, 37–55. URL: http://link.springer.com/article/10.1007/s40304-015-0050-5. 25

LOGG, A., WELLS, G. N., AND HAKE, J. 2012. *DOLFIN: a C++/Python Finite Element Library*. Springer. 31

LU, L., SHARF, A., ZHAO, H., WEI, Y., FAN, Q., CHEN, X., SAVOYE, Y., TU, C., COHEN-OR, D., AND CHEN, B. 2014. Build-to-last: Strength to weight 3d printed objects. *ACM Trans. Graph. 33*, 4 (July), 97:1–97:10. URL: http://doi.acm.org/10.1145/2601097.2601168, doi:10.1145/2601097.2601168. 19, 21, 32, 33

LUO, L., BARAN, I., RUSINKIEWICZ, S., AND MATUSIK, W. 2012. Chopper: Partitioning models into 3d-printable parts. *ACM Trans. Graph. 31*, 6 (Nov.), 129:1–129:9. URL: http://doi.acm.org/10.1145/2366145.2366148, doi:10.1145/2366145.2366148. 20

NOCEDAL, J., AND WRIGHT, S. 2006. *Numerical Optimization*, 2nd ed. Springer. 28

PARLETT, B. N. 1998. *The Symmetric Eigenvalue Problem*. Prentice-Hall, Inc. 25, 27

PRÉVOST, R., WHITING, E., LEFEBVRE, S., AND SORKINE-HORNUNG, O. 2013. Make it stand: Balancing shapes for 3d fabrication. *ACM Trans. Graph. 32*, 4 (July), 81:1–81:10. URL: http://doi.acm.org/10.1145/2461912.2461957, doi:10.1145/2461912.2461957. 20

ROZVANY, G. I. 1989. *Structural design via optimality criteria*. Springer. 22

ROZVANY, G. I. 2009. A critical review of established methods of structural topology optimization. *Structural and Multidisciplinary Optimization 37*, 3, 217–237. URL: http://link.springer.com/article/10.1007/s00158-007-0217-0. 22, 23

SMITH, J., HODGINS, J., OPPENHEIM, I., AND WITKIN, A. 2002. Creating models of truss structures with optimization. *ACM Trans. Graph. 21*, 3 (July), 295–301. URL: http://doi.acm.org/10.1145/566654.566580, doi:10.1145/566654.566580. 21

STAVA, O., VANEK, J., BENES, B., CARR, N., AND MĚCH, R. 2012. Stress relief: Improving structural strength of 3d printable objects. *ACM Trans. Graph. 31*, 4 (July), 48:1–48:11. URL: http://doi.acm.org/10.1145/2185520.2185544, doi:10.1145/2185520.2185544. 19, 20

TAKEZAWA, A., NII, S., KITAMURA, M., AND KOGISO, N. 2011. Topology optimization for worst load conditions based on the eigenvalue analysis of an aggregated linear system. *Computer Methods in Applied Mechanics and Engineering 200*, 25, 2268–2281. URL: http://www.sciencedirect.com/science/article/pii/S0045782511001137. 21

UMETANI, N., AND SCHMIDT, R. 2013. Cross-sectional structural analysis for 3d printing optimization. In *SIGGRAPH Asia 2013 Technical Briefs*, ACM, New York, NY, USA, SA '13, 5:1–5:4. URL: http://doi.acm.org/10.1145/2542355.2542361, doi:10.1145/2542355.2542361. 21

WANG, C. C., AND CHEN, Y. 2013. Thickening freeform surfaces for solid fabrication. *Rapid Prototyping Journal 19*, 6, 395–406. URL: http://www-bcf.usc.edu/~yongchen/Research/RPJThickening.pdf. 29

WANG, H., CHEN, Y., AND ROSEN, D. W. 2005. A hybrid geometric modeling method for large scale conformal cellular structures. In *ASME 2005 International Design Engineering Technical Conferences and Computers and Information in Engineering Conference*, American Society of Mechanical Engineers, 421–427. URL: http://www-bcf.usc.edu/~yongchen/Research/HybridModeling.pdf. 21

WANG, W., WANG, T. Y., YANG, Z., LIU, L., TONG, X., TONG, W., DENG, J., CHEN, F., AND LIU, X. 2013. Cost-effective printing of 3d objects with skin-frame structures. *ACM Trans. Graph. 32*, 6 (Nov.), 177:1–177:10. URL: http://doi.acm.org/10.1145/2508363.2508382, doi:10.1145/2508363.2508382. 19, 20, 21, 26, 28

XIE, Y. M., AND STEVEN, G. P. 1997. *Basic evolutionary structural optimization*. Springer. 22

YAN, D.-M., LÉVY, B., LIU, Y., SUN, F., AND WANG, W. 2009. Isotropic remeshing with fast and exact computation of restricted voronoi diagram. In *Computer Graphics Forum*, Wiley Online Library, 1445–1454. URL: http://research.microsoft.com/en-us/UM/people/yangliu/publication/Isotropic%20Remeshing%20with%20Fast%20and%20Exact%20Computation%20of%20Restricted%20Voronoi%20Diagram.pdf. 23

YAN, D.-M., WANG, W., LÈVY, B., AND LIU, Y. 2010. Efficient computation of 3D clipped Voronoi diagram. In *6th International Conference on Geometric Modeling and Processing (GMP 2010)*, Springer, 269–282. URL: http://research.microsoft.com/en-us/UM/people/yangliu/publication/Efficient%20Computation%20of%203D%20Clipped%20Voronoi%20Diagram.pdf. 26, 27

ZHANG, X., XIA, Y., WANG, J., YANG, Z., TU, C., AND WANG, W. 2015. Medial axis tree - an internal supporting structure for 3d printing. *Computer Aided Geometric Design 35*, 149–162. URL: http://dx.doi.org/10.1016/j.cagd.2015.03.012. 19

ZHOU, Q., PANETTA, J., AND ZORIN, D. 2013. Worst-case structural analysis. *ACM Trans. Graph. 32*, 4 (July), 137:1–137:12. URL: http://doi.acm.org/10.1145/2461912.2461967, doi:10.1145/2461912.2461967. 21, 25, 30

Author Contact Information

Tuanfeng Y. Wang
University College London
tuanfeng.wang@cs.ucl.ac.uk

Yuan Liu
University of Science and
Technology of China

Xuefeng Liu
Niigata University

Zhouwang Yang
University of Science and
Technology of China
yangzw@ustc.edu.cn
(Corresponding author)

Dongming Yan
National Laboratory of
Pattern Recognition
Institute of Automation
Chinese Academy of Sciences

Ligang Liu
University of Science and
Technology of China

Tuanfeng Y. Wang, Yuan Liu, Xuefeng Liu, Zhouwang Yang, Dongming Yan, and Ligang Liu, Global Stiffness Structural Opt. for 3D Printing Under Unknown Loads, *Journal of Computer Graphics Techniques (JCGT)*, vol. 5, no. 3, 18–38, 2016
http://jcgt.org/published/0005/03/02/

Received:	2015-06-05		
Recommended:	2016-02-22	Corresponding Editor:	Bernd Bickel
Published:	2016-08-11	Editor-in-Chief:	Marc Olano